Fabrication and Analysis of Thermally Invariant Smart Composites via Ultrasonic Additive Manufacturing

Joshua D. Pritchard

Smart Materials and Structures Laboratory

Department of Mechanical and Aerospace Engineering

The Ohio State University

Abstract

Ultrasonic additive manufacturing (UAM), a form of 3D printing based on ultrasonic metal welding, is a fabrication technique that is rapidly altering the development of new components within the research and commercial industries. Through the use of piezoelectric boosters, vibrating at 20 kHz, and the application of normal forces in excess of 5000 Newtons, thin metal foils can be welded in a fusionless, low-temperature process to produce bulk structures. Because of its low-temperature, UAM provides the opportunity to embed thermally sensitive materials, such as nickel-titanium (NiTi), a shape memory alloy. NiTi exhibits a shape change as it undergoes thermally-induced crystallographic phase transformation between martensite, the low-temperature phase, and austenite, the high-temperature phase. During phase transformations, NiTi can recover up to 8% elastic strain and have a change in elastic modulus of 100%. When embedded, the strain recovery of NiTi can be used to counteract the thermal expansion of the matrix material—specifically aluminum in this study—for the purpose of producing components with low coefficients of thermal expansion (CTE) while keeping the weight at a minimal level. The work herein covers the design, fabrication, and characterization of Al-NiTi composites to aid in the development of a composite that has a coefficient of thermal expansion at, or below, 5 $\mu\epsilon$/°C. A composite is produced that has a CTE of 13.83 $\mu\epsilon$/°C; a 40.4% decrease as compared to Al alone. In addition, electrical resistivity measurements in the longitudinal direction and thermal diffusivity measurements in the out-of-plane directions are presented.

I. Introduction

Ultrasonic additive manufacturing (UAM) is a recent manufacturing process that utilizes ultrasonic welding in conjunction with subtractive milling operations to produce bulk parts with complex and internal geometries. The process in carried out by applying the vibrating energy of piezoelectric transducers to thin metal foils, Figure 1. A horn, or sonotrode, is used to transfer vibrations and apply a downward normal force between the structure being fabricated and the foil being welded. By successively welding the foils and using periodic machining operations, a 3D part can be achieved. Unique to the UAM process, all bonding of the foils is done through a low-temperature, fusionless process, meaning that no melting takes place. Because of this characteristic, UAM provides the opportunity to embed thermally sensitive materials, such as shape memory alloys (SMA), in a metal matrix.

Shape memory alloys are metals that have the ability to recover large amount of strain, or deformations—on the order of 8%—through phase changes. Nickel-titanium (NiTi) in

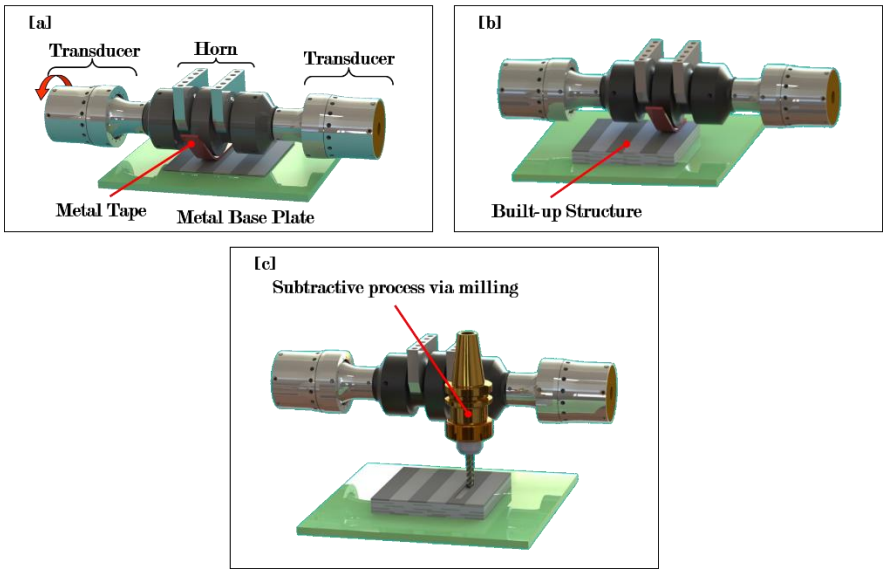

Figure 1 - Ultrasonic additive manufacturing process. [a] Welding of first metal tape/foil layer to base plate by horn vibrating at ultrasonic frequencies, [b] building of structure by successively welding layers of metal foils, and [c] producing specific part geometries through the use of period machining operations. Renderings courtesy of Fabrisonic.

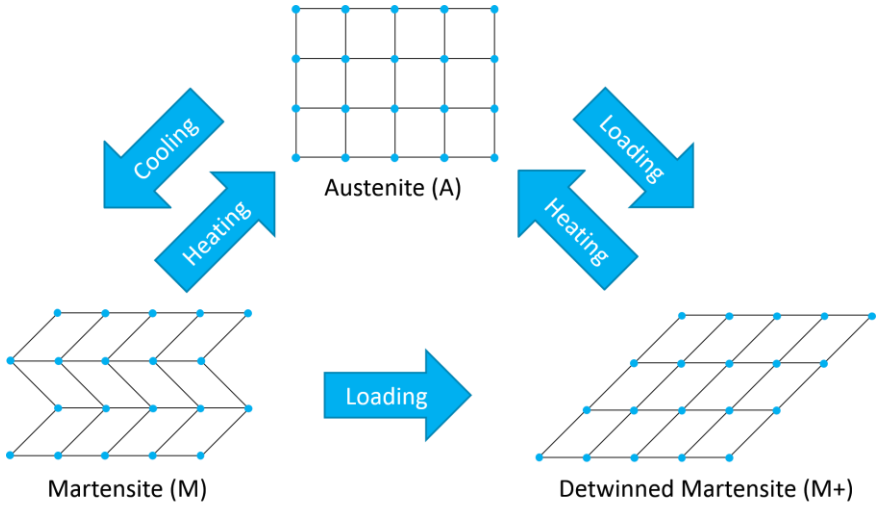

Figure 2 - The phase transformation cycle of NiTi. The cycle begins in the twinned martensite phase, M, where the material can be loaded to form detwinned martensite, M+. By applying heat, the detwinned martensite transforms into austenite and recovers the deformation caused via detwinning. Cooling the austenite returns the material to martensite again. Direct heating of the martensite can also cause the transformation to austenite. Finally, austenite can transform to detwinned martensite by inducing strain.

particular recovers these strains as the material transforms between a face-centered cubic martensite phase and a body-centered cubic austenite phase. In addition, the martensite can take the form of a self-accommodating twinned phase or a detwinned phase. The transformation between these phases and forms occurs when the material is heated or cooled and through the application of external loads, Figure 2.

Through the use of ultrasonic additive manufacturing, a low-temperature process, the embedding of nickel-titanium is possible despite its strong dependence on temperature. By embedding NiTi fibers in a metal matrix, properties of both the fibers and the matrix contribute to the overall performance of the composite. Within this work, the coefficient of thermal expansion (CTE) of the composite is the focus, with minor emphasis on electrical properties.

Due to its ability to recover large deformations, NiTi fibers were chosen to offset the expansion of an aluminum (Al) matrix to produce a composite with an overall low CTE (at or below 5 μm/°C). The use of Al for the matrix was chosen for its high strength to weight ratio,

Table 1 - Material properties of Invar and aluminum. Material data from matweb.com.

Material	Density	CTE
Invar	8.05 g/cc	1.30 μϵ/°C
Aluminum	2.70 g/cc	23.60 μϵ/°C

which makes it valuable in light-weighting applications often found in the aerospace and automotive industries. By making the composite, current components made out of iron-based Invar® could be replaced with parts that are approximately 1/3 the density, Table 1.

II. Design and Fabrication

The design of the Al-NiTi composite within this study was done through the use of a numerical model developed by Hahnlen [2], which utilizes material property data from the constituent materials to determine the overall performance of the composite. The property data is applied to

$$\epsilon_{\text{comp}} = \epsilon_{\text{matrix}} = \left(\sigma_{\text{matrix}} - \sigma_{\text{matrix,o}}\right)/E_{\text{matrix}} + \alpha_{\text{matrix}}(T - T_{\text{o}}) = \left(\sigma_{\text{fiber}} - \sigma_{\text{fiber,o}}\right)/E_{\text{fiber}} + \alpha_{\text{fiber}}(T - T_{\text{o}}) + \epsilon_L\left(\xi_{\text{stress}} - \xi_{\text{stress,o}}\right) = \epsilon_{\text{fiber}} \quad (1)$$

where E, α, and ϵ_L are the elastic modulus, coefficient of thermal expansion, and maximum recoverable strain in the NiTi respectively; ϵ, σ, T, and ξ correspond to the strain, stress, temperature and martensitic volume fractions. A volume fraction of NiTi to achieve the desired CTE from 23 to 100°C was calculated to be 17.2%, Figure 3. This was determined by applying the material property data for the aluminum and the specific NiTi used within this composite to the model. Based on this design, the prestressed NiTi material should be able to

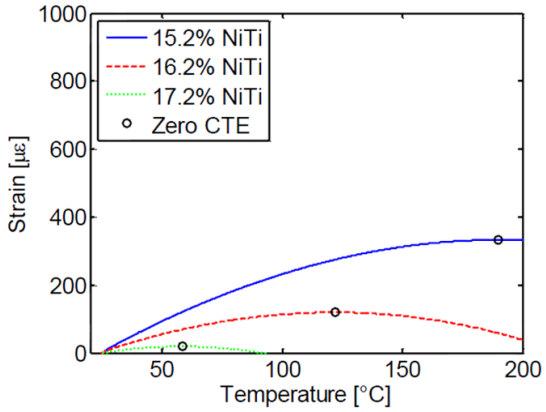

Figure 3 - Strain-matching numerical model results for Al-NiTi composite performance [2].

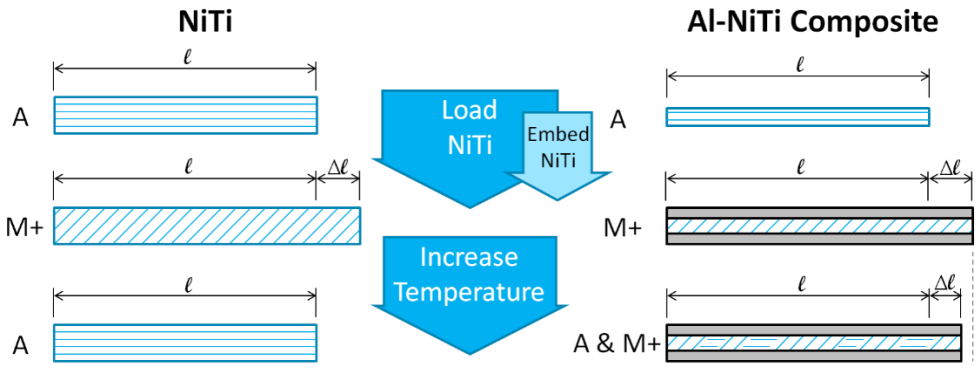

Figure 4 - Diagram of Al-NiTi composite theory.

recover the initial strain as the aluminum expands, Figure 4, resulting in the reduction of the overall CTE.

Production of the Al-NiTi composite was done using a custom fixture and clamping system, which allowed the NiTi ribbons to be held in tension as they were embedded. The placement of the ribbons within the composite was controlled by milling channels, Figure 5. Placement of the ribbons was determined by the need to create planes of symmetry within the part, both vertical and horizontal, to reduce the possibility of bending occurring due to unequal forces on opposite sides of the composite and ensuring the ribbons were distributed evenly throughout the composite to counter the expansion of the aluminum. Welding parameters were determined based on a study performed by Wolcot al. [3], Table 2.

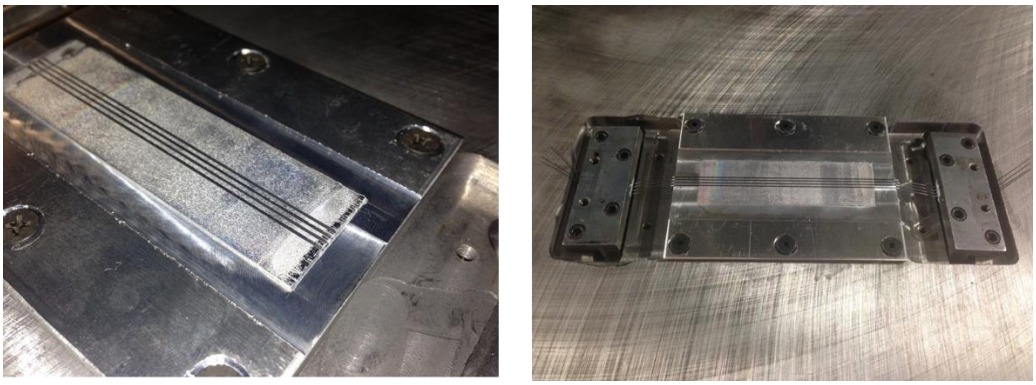

Figure 5 - Production of Al-NiTi composite. [a] Composite with channels milled for NiTi ribbons and [b] prestrained NiTi ribbons held in place before encapsulation layer welded.

Table 2 - Weld parameters used for fabrication Al-NiTi composite [3].

Parameter	Level
Amplitude	32.76 µm
Weld Speed	200 in/min
Weld Force	5000 N

III. Testing

Thermal cycling, electrical resistivity, and thermal diffusivity tests were conducted on the composite produced according to the model and procedure stated previously. The thermal tests were carried out in a custom thermal chamber that allowed for testing of the composite and an aluminum reference sample simultaneously, Figure 6. To measure the free thermal expansion

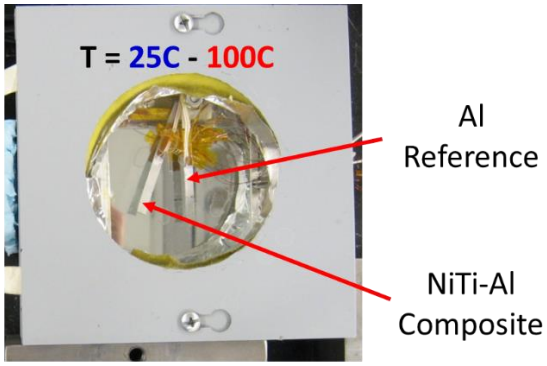

Figure 6 - Thermal chamber for thermal cycling of Al-NiTi composites versus an aluminum reference.

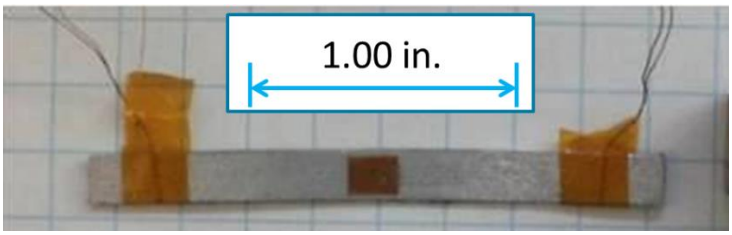

Figure 7 - Sample for 4-wire test method of electrical resistivity.

of each piece, strain gauges, (Micro-measurements® WK-13-013CG-350) were applied to the top and bottom surfaces of each piece while J-type thermal couples measured each sample's temperature. The tests were conducted six times over the 23 to 100°C range.

Electrical resistivity, tests were performed using the 4-wire method to determine the flow of electrons through the composite along the longitudinal direction, the direction in which the NiTi ribbons travel, Figure 7. An initial baseline study was carried out using a piece of Al-3003. The measurements were performed on an insulated surface to ensure all recorded values were that of the composite and not from the supporting surface. A nanovoltmeter and precision current source were used to ensure accuracy of the measurements.

Finally, thermal diffusivity measurements were conducted on the composite using an Anter Flashline-5000 diffusivity meter. Thermal diffusivity is the measurement of how fast heat can flow through an area. This type of measurement was performed in the out-of-plane direction, Figure 8. The measurement is performed by pulsing a laser at the upper side of a sample and measuring the time it takes to see a rise in the heat signature on the bottom side, Figure 9.

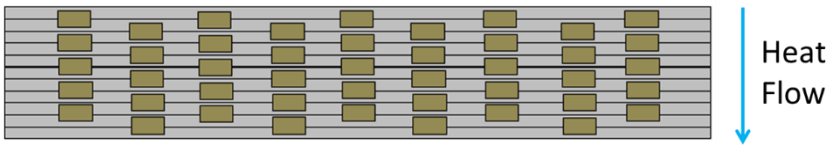

Figure 8 - Diagram of the direction in which the thermal diffusivity was measured for the Al-NiTi in the out-of-plane direction.

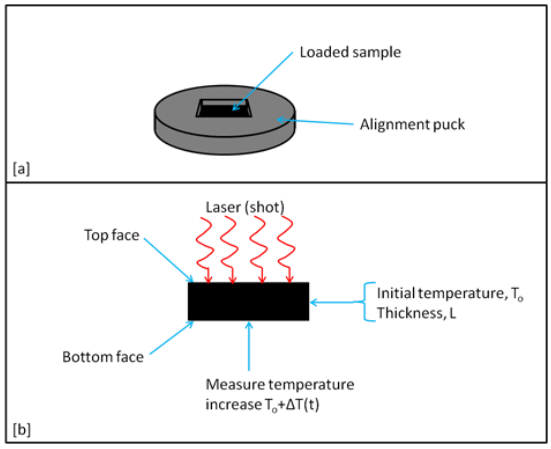

Figure 9 - Diagram of how thermal diffusivity measurement systems works.

IV. Results

From the results of the thermal tests, a strain temperature plot was produced, where the slope of each line provides the CTE at a given temperature, Figure 10. The result of 6 cycles provided an average CTE for the composite of 13.83 $\mu\epsilon$/°C, a 40.4% decrease from aluminum alone. However, the result for the composite was still greater than the desired CTE of 5 $\mu\epsilon$/°C or less. Further investigation determined that the composite's CTE was the expected CTE if the NiTi ribbons were not subjected to any initial prestrain. This implies that the composite followed the basic rule of mixtures,

$$\alpha_{\text{comp}} = \alpha_{\text{fiber}}\nu + \alpha_{\text{matrix}}(1-\nu), \tag{2}$$

where ν is the volume fraction of the fibers within the composite. The only cycle that does not seem to follow the rule of mixtures is the first cycle, where a large amount of strain recovery is present from 70 to 100°C suggesting that the NiTi ribbons did not begin to transform until higher than anticipated temperatures were reached. Furthermore, once the transformation did begin to take place, the matrix was unable to withstand the stresses at the fiber-matrix interface and yielded.

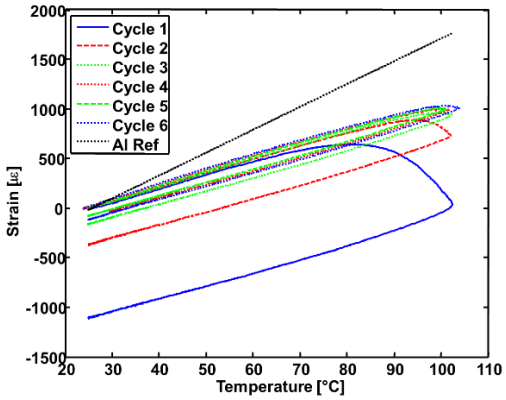

Figure 10 - Results of thermal tests of Al-NiTi composite over 6 cycles for the temperature range of 25 to 100°C.

The electrical resistivity measurement conducted on the Al-NiTi composite yielded a resistance of 4.94 μΩ-m in the longitudinal direction. Comparing this result to a theoretical value from a resistance model, Figure 11, the two differ by 16.2%, where the theoretical value was calculated to be 4.25 μΩ-m.

The thermal diffusivity measurements in the out-of-plane direction resulted in a value of 0.046 cm^2/s, a value close to that of NiTi, 0.048 cm^2/s. The actual lower value in thermal diffusivity of the composite is thought to be the result of the fibers absorbing the heat energy for the purpose of transformation and the existence of micro air pockets around the fibers within the matrix.

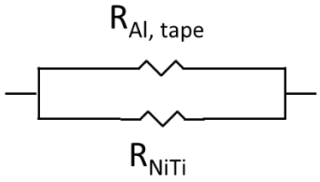

Figure 11 - Resistance model used for prediction of electrical resistivity of the Al-NiTi composite.

V. Conclusion and Future Work

Current work on this project has shown promise in the ability to embed NiTi fibers within an aluminum matrix using UAM. In addition, the first cycle of thermal testing provided

evidence that a lower CTE than aluminum can be achieved with a composite, however attention needs to be given to understanding how the interface between the fiber and the matrix can be improved and the maximum stress that it can withstand. The measurements for electrical resistivity and thermal diffusivity also provided results for the longitudinal and out-of-plane directions, respectively.

To ensure continued understanding in this area of work, an investigation into the strength of the fiber-matrix interface will be conducted. Scaling up the volume of the composites will also take place to allow the measurement of electrical resistivity and thermal diffusivity in all three directions, longitudinal, out-of-plane and transverse.

Acknowledgements

The author would like to acknowledge the member organizations of the Smart Vehicle Concepts Center (www.SmartVehicleCenter.org) a National Science Foundation Industry/ University Cooperative Research Center (I/UCRC). The support and contributions of Prof. Marcelo Dapino (project advisor), Adam Hehr, Cameron Benedict, and Walter Green are acknowledged. An additional acknowledgement to the Thermal Materials Lab at The Ohio State University for assistance with performing measurements and use of equipment.

References

[1] P. Evans, M. Dapino, R. Hahnlen and J. Pritchard. "Dimensionally Stable Optical Metering Structures With NiTi Composites Fabricated Through Ultrasonic Additive Manufacturing." *ASME 2013 Conference on Smart Materials, Adaptive Structures and Intelligent Systems*. American Society of Mechanical Engineers, 2013.

[2] R. Hahnlen. *Characterization and Modeling of Active Metal-Matrix Composites with Embedded Shape Memory Alloys*. Ph.D. dissertation, The Ohio State University, 2012.

[3] P.J. Wolcott, A. Hehr, and M.J. Dapino. "Optimal welding parameters for very high power ultrasonic additive manufacturing of smart structures with aluminum 6061 matrix." *SPIE Smart Structures and Materials & Nondestructive Evaluation and Health Monitoring*. International Society for Optics and Photonics, 2014.